THE JOURNAL OF PHYSICAL CHEMISTRY LETTERS
A JOURNAL OF THE AMERICAN CHEMICAL SOCIETY

pubs.acs.org/JPCL

Letter

Bimolecular Generation of Excitonic Luminescence from Dark Photoexcitations in Ruddlesden–Popper Hybrid Metal-Halide Perovskites

Matthias Nuber, Daniel Sandner, Timo Neumann, Reinhard Kienberger, Felix Deschler,* and Hristo Iglev*

Cite This: *J. Phys. Chem. Lett.* 2021, 12, 10450–10456

Read Online

ACCESS | Metrics & More | Article Recommendations | Supporting Information

ABSTRACT: The nature of photoexcitations in Ruddlesden–Popper (RP) hybrid metal halide perovskites is still under debate. While the high exciton binding energy in the hundreds of millielectronvolts indicates excitons as the primary photoexcitations, recent reports found evidence for dark, Coulombically screened populations, which form via strong coupling of excitons and the atomic lattice. Here, we use time-resolved mid-infrared spectroscopy to gain insights into the nature and recombination of such dark excited states in $(BA)_2(MA)_{n-1}Pb_nI_{3n+1}$ (n = 1,2,3) via their intraband electronic absorption. In stark contrast to results in the bulk perovskites, all samples exhibit a broad, unstructured mid-IR photoinduced absorbance with no infrared activated modes, independent of excitonic confinement. Further, the recombination dynamics are dominated by a bimolecular process. In combination with steady-state photoluminescence experiments, we conclude that screened, dark photoexcitations act as a population reservoir in the RP hybrid perovskites, from which nongeminate formation of bright excitons precedes generation of photoluminescence.

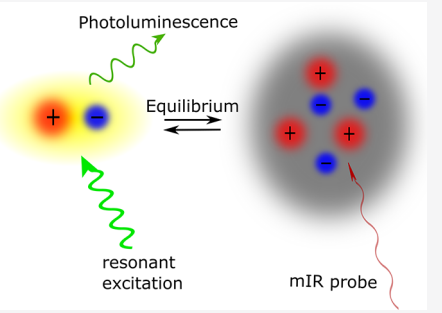

Organometallic halide perovskites have been suggested for a wide range of optoelectronic applications.[1−6] Their broad application range results from their unique charge carrier properties. In most three-dimensional (3D) perovskites, a very small exciton binding energy allows an immediate separation of the charge carriers into free electrons and holes. On the perovskite structure, these charges are stabilized due to the formation of polarons by a structural reaction of the lattice to the additional charge being present. The presence of these "large polarons" has been associated with the extraordinary properties of perovskite materials.[7−13] While 3D perovskites have many favorable properties and have already been investigated in much detail, degradation effects pose a serious obstacle for widespread application.[14,15] These effects can lead to permanent damage by ion movement and segregation of the halides. Polaron formation has been associated with some of these processes.[16]

The insertion of additional, larger organic molecules as spacers between layers of inorganic lead halide octahedra leads to two-dimensional (2D) Ruddlesden–Popper structures. These isolated layers have a reduced dimensionality and form quantum-well-like systems with additional degrees of freedom. Furthermore, these materials exhibit an improved stability due the isolation of the functional layers by the spacer molecules acting as a diffusion barrier.[17]

Popular 2D perovskites have been derived from the MAPI (methylammonium lead iodide) prototypical 3D perovskite system. Insertion of longer organic cations such as butylammonium (BA) leads to layers of MAPI of a defined thickness, resulting in $BA_2(MA)_{n-1}Pb_nI_{3n+1}$ (BAPI) with thickness n. These systems can be considered as prototypical 2D perovskites.

While 3D perovskites are often regarded as mainly polaronic with strong coupling to lattice motions, for 2D perovskites, the exciton binding energy (E_b) usually is much higher, leading to a characterization as being of excitonic nature.[18]

In recent years, several publications investigated the charge-carrier behavior in 2D hybrid perovskites. Many of these studies used time-resolved photoluminescence (TRPL) measurements to monitor the recombination of excitons over time using multiexponential fits as a model. The different fit components are then often related to free and trapped exciton recombination.[19,20]

Contrary to TRPL experiments, vis–vis transient absorption (vis-TA) measurements are sensible to all charge carriers present on the sample. Recombination components missing in

Received: September 21, 2021
Accepted: October 18, 2021
Published: October 21, 2021

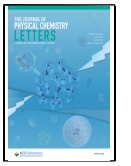

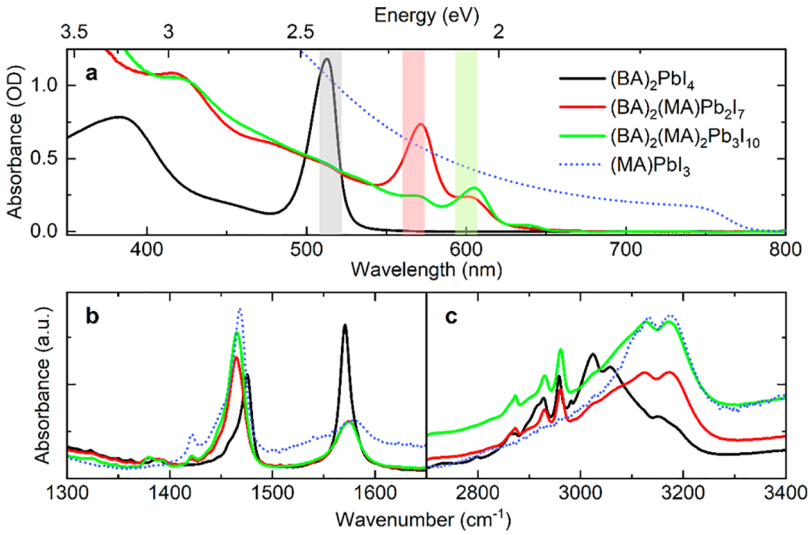

Figure 1. (a) UV−vis spectrum of $(BA)_2(MA)_{n-1}Pb_nI_{3n+1}$ (n = 1, 2, 3) and $(MA)PbI_3$ (n = ∞) for comparison. The excitation wavelength in the time-resolved mIR measurements is highlighted by a color bar. (b,c) Infrared spectrum of $(BA)_2(MA)_{n-1}Pb_nI_{3n+1}$ (n = 1, 2, 3) and $(MA)PbI_3$ (n = ∞) for comparison in the "fingerprint" region (b) and around 3000 cm^{-1} (c).

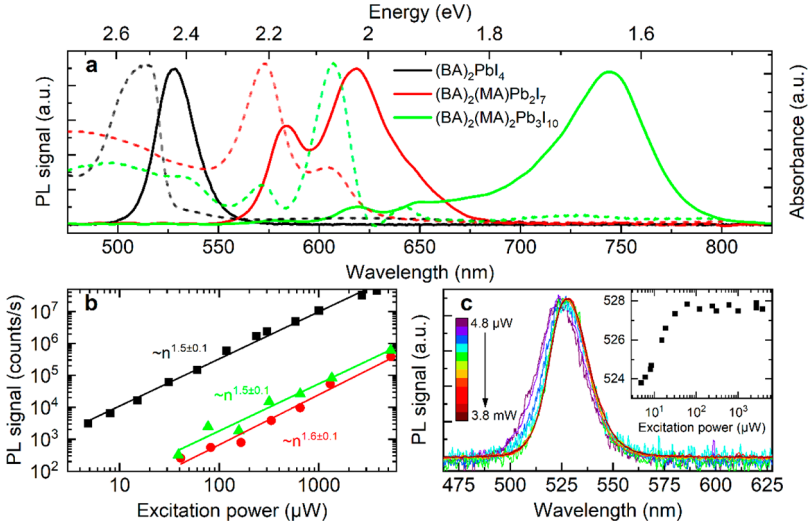

Figure 2. (a) Normalized photoluminescence spectra of $(BA)_2(MA)_{n-1}Pb_nI_{3n+1}$ (n = 1, 2, 3) with corresponding normalized absorption spectra (dashed lines) for comparison. (b) Excitation power dependency of the integrated PL signal. Color code as in (a). (c) Red-shift of the $(BA)_2PbI_4$ (n = 1) PL signal with increasing excitation density; the inset shows the peak wavelength as obtained from a Gaussian fit.

comparable TRPL measurements are often associated with nonradiative recombination paths. Nevertheless, the main fit model so far used in literature to analyze the vis-TA data is multiexponential, assuming a dominant monomolecular exciton mechanism[21] with possible additional bimolecular effects due to EEA.[22]

Combining and comparing data from TRPL and vis-TA experiments proves to be complex. Usually TRPL and vis-TA measurements are conducted on different experimental setups, which can lead to uncertainties regarding the excitation density and the exact sample position investigated.

In a very recent publication, Simbula et al.[23] aimed to overcome these obstacles using an ultrafast tandem spectroscopy approach, combining both measurement techniques in a single experimental setup. They found that for 2D perovskites, $(BA)_2PbI_4$ in this case, the bright luminescent excitons are in an equilibrium with an additional dark species forming the majority population. They interpreted their findings based on polarons being formed on the 2D perovskites, even though the exciton binding energy of these systems significantly exceeds k_BT at room temperature, which hinders free charge-carrier formation. They argued that the exciton and polaron population are in an equilibrium with the probability of exciton formation being reduced as the polarons are energetically stabilized and have an increased mass compared to free carriers.

Strongly screened charge carriers usually have smaller binding energies on the order of tens of meV.[24−26] Our transient absorption spectroscopy in the mid-IR (mIR-TA) can therefore monitor their electronic transitions directly.[27,28]

Here, we present the dynamics of the dark majority population in $(BA)_2(MA)_{n-1}Pb_nI_{3n+1}$ perovskites with different thicknesses (n = 1, 2, 3) using mIR-TA on the picosecond time scale. We find a dominant dark population reservoir, which recombines via a bimolecular recombination process for all samples investigated. They thereby form bright excitons, which

https://doi.org/10.1021/acs.jpclett.1c03099
J. Phys. Chem. Lett. 2021, 12, 10450−10456

cause the photoluminescence in these samples. The decrease in exciton binding energy with increasing layer size appears to have little influence on the population of these screened charge carriers.

2D Ruddlesden−Popper perovskites are characterized by a band gap signal at higher energies and a distinct exciton peak as the lowest optical resonance. That exciton resonance is associated with the 2D nature of photoexcitations in these materials. In Figure 1a, the absorption spectra of the samples used for this publication are shown. The trend toward a lower band gap and exciton energy with increasing active layer thickness is well-visible. In particular, the exciton resonance peak moves from around 515 nm for $n = 1$ over 567 nm ($n = 2$) to around 600 nm for the $n = 3$ variant. In addition, the peak intensity weakens with increasing active layer thickness. These findings are in good agreement with spectra reported in literature.[29,30]

Additional infrared spectra, presented in Figure 1b,c, show the distinct vibrational signature of these samples, which originate from their organic cations. A more detailed analysis of the infrared spectra can be found in the Supporting Information.

Analyzing the photoluminescence (PL) behavior of perovskites allows investigating the key recombination mechanisms of photoexcitations in these systems. PL spectra can additionally provide information on further states, such as biexcitons.[31,32]

In Figure 2a, the photoluminescence spectra of the samples are presented. While the single-layer $n = 1$ variant shows a single peak around 528 nm, the quasi-2D variants with $n = 2$ and $n = 3$ show a more complex PL spectrum. Similarly to their UV−vis absorption, additional signals occur due to other phases being present in the samples. In the absorption spectrum, these phases have a negligible signal strength compared to the main layer thickness. Nevertheless, for the exciton recombination, which is at the physical origin of the photoluminescence in 2D perovskites, a different behavior can be observed. As already described in the literature, photoexcitations tend to transfer to the large-n phases, where they have a smaller exciton binding energy.[33,34] That leads to PL spectra where additional peaks at lower photon energy are comparatively more dominant. This effect has been described with a wide range of characteristic times from some picoseconds[33] up to nanoseconds.[34] As there is no effect on this time scale apart from the bimolecular recombination described later, we conclude that these effects occur later to the effects described in this article. In the $n = 1$ variant, we additionally find that with very small excitation power, the spectrum of the photoluminescence shifts to smaller wavelengths as demonstrated in Figure 2c. A detailed discussion of this effect may be found in the Supporting Information.

Apart from spectral changes, the relation between the integrated photoluminescence signal and the excitation density enables insights into the charge-carrier recombination mechanisms. In principle, the PL intensity I follows a power law $I \propto N^l$ with N being the charge-carrier density, which approximately is linearly dependent on the excitation density, and l being the power index. In the literature, an index of $l = 1$ has been associated with a monomolecular recombination behavior, which is characteristic of a purely excitonic process.[35] For a bimolecular process, which would be characteristic for a polaronic recombination, an index of $l = 2$ can be deviated.[36] In the samples investigated here, we find power exponents of approximately $l = 1.5$ for all three structures as shown in Figure 2b. For perovskite samples, a wide range of power exponents between $l = 1$ and $l = 2$ has been reported. While some reports showed a clear linear relationship between excitation fluence and the initial PL intensity for quasi-2D perovskites indicating an emission from an excitonic state[37,38] and a power exponent of $l = 2$ for 3D perovskites connected to a free carrier emission,[36,39] other experiments show a more complex picture. Values on the order of $l = 1.5$, like our findings, have been associated with a variety of effects. In many cases, the deviation from a purely excitonic behavior was associated with additional trap states.[40−42] Although the plethora of influencing factors make a concluding assignment of a certain recombination mechanism to a specific power coefficient rather speculative, it is apparent that a more complex view of the exciton signal in the systems investigated here is required.[18] In particular, possible dark states, which do not recombine radiatively, can influence the exciton population; their recombination behavior therefore needs to be considered to obtain a realistic description of the photophysics in these materials.

Time-resolved spectroscopy on perovskite samples usually is performed by either transient absorption spectroscopy in the visible (vis-TA), time-resolved PL (TRPL) spectroscopy, or a combination of both. Nevertheless, to study polaronic charge carriers with a strong electron−phonon coupling directly, monitoring their electronic absorption, mid-infrared time-resolved spectroscopy proves to be a valuable tool.[27,43] In our experiments, we find very broad, unstructured absorption features arising within our time resolution of approximately 0.5 ps upon excitation of the samples at their characteristic exciton resonance. Contrary to reports of the three-dimensional MAPI perovskite,[28,44] there are no signs of polaronic infrared activated vibrations close to the ground-state vibrational modes in the spectroscopic "fingerprint" region. In addition to the spectra used for the analysis in Figure 3 (the spectra are presented in the Supporting Information as Figures S3 − S5), we further extended the probe region for the $(BA)_2(MA)_2Pb_3I_{10}$ sample to higher probe frequencies up to 2300 cm^{-1} without encountering relevant changes in the signal. Our probe energy is in the energy range of 156 to 195 meV for all samples with additional measurements for the $n = 3$ variant reaching up to 285 meV. Calculations in literature assume the exciton binding energy of the three variants investigated to increase from the probe region in this experiment for the $n = 3$ case to much higher energies for the $n = 2$ and $n = 1$ case.[45] The spectral shapes we found in our experiments show no relevant difference between the samples. This suggests that the charge carriers observed in our experiments are of the same nature independent of the active layer thickness. As the exciton binding energy changes significantly between the samples, an excitonic origin of the sample should lead to relevant differences for samples with exciton binding energies below or close to the MIR probe energy compared to the samples in which the exciton is bound much stronger. In particular, the occurrence of photoinduced absorption peaks around the exciton binding energy and due to transitions within the exciton levels could be expected if the infrared signal was excitonic. The very broad spectra with no clear structure for all three variants with their varying exciton binding energy lack such excitonic signatures. They point to an electronic absorption, in which a bound carrier can be excited to the conduction band over a broad energy range as the probe energy exceeds its electronic binding energy. We therefore

https://doi.org/10.1021/acs.jpclett.1c03099
J. Phys. Chem. Lett. 2021, 12, 10450−10456

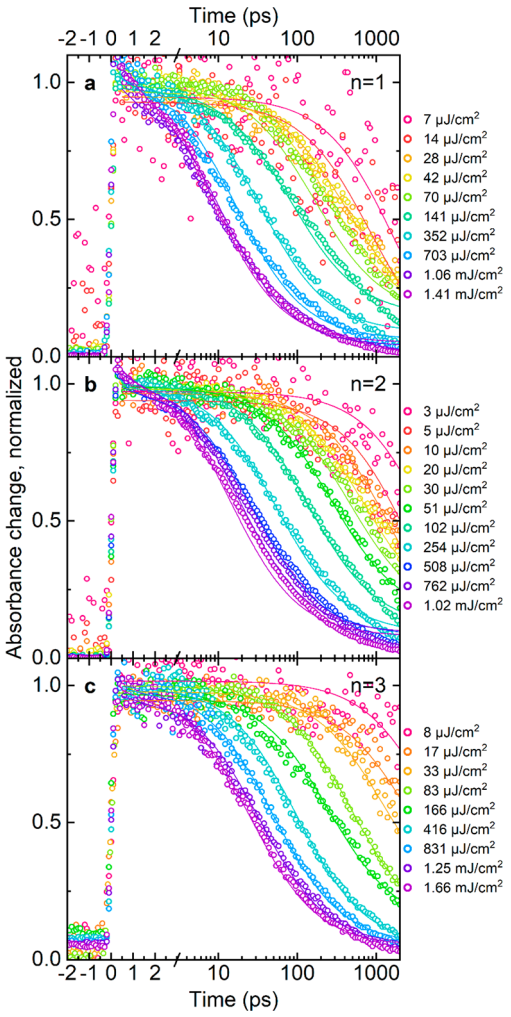

Figure 3. Normalized recombination dynamics for $(BA)_2(MA)_{n-1}Pb_nI_{3n+1}$ (n = 1, 2, 3) in (a–c), respectively, together with a bimolecular fit. The data is averaged from 64 detector pixels covering a spectral region from 1257 to 1356 cm^{-1}.

conclude that the signal we find in the mid-infrared is not of a purely excitonic nature but that it rather points to a state in which Coulombic polaronic screening reduces the binding energies of the photoexcitations considerably.[26,46]

Evaluating the picosecond recombination behavior of the samples over multiple excitation densities as shown in Figure 3a–c, we find a distinctive bimolecular behavior. In addition, at very high excitation densities, a higher-order mechanism, such as Auger recombination, might be present at very short time scales. Within our time resolution of approximately 0.5 ps, we do not observe delayed processes, and the maximum absorbance change is reached immediately. We find that for the smallest exciton densities around 10 $\mu J/cm^2$, corresponding to initial charge-carrier densities on the order of 5×10^{17} cm^{-3}, very long carrier lifetimes up to nanoseconds can be observed. To further evaluate the data, we fitted a bimolecular recombination model to the data: $n(t) = A\frac{n_0}{n_0 k_2 t + 1} + y_0$. Here, we use a rate equation model, which is well-established in the literature,[47,48] and its bimolecular solution for a global fit with a shared bimolecular recombination constant k_2 (calculations of the initial charge-carrier density n_0 can be found in the Supporting Information). Due to the limited time scale of 2 ns investigated here, an additional monomolecular component cannot be supported by the data (see SI Figure S2). We find that the recombination constants are similar for all three samples with the fitted k_2 being $(7.5 \pm 0.3)*10^{-10}$, $(9.0 \pm 0.3)*10^{-10}$, and $(6.7 \pm 0.2)*10^{-10}$ cm^3/s for the n = 1, 2, 3 variants, respectively. Although the exact fit values of k_2 need to be considered with some reserve, in particular when comparing them with other measurements from literature, due to large interdependence with the initial charge-carrier density n_0, it is clear that the bimolecular recombination rates appear not to differ massively with changing active layer thickness. The k_2 values obtained from the fit are of similar order as values reported for MAPI ($n = \infty$)[28] or other 2D perovskites.[49] In contrast to measurements by Chen et al.[49] with $(PEA)_2(MA)_{n-1}Pb_nI_{3n+1}$, we did not find a distinct decrease in the k_2 from n = 1 to the n = 2, 3 variants. This further strengthens the assumption that the photoexcitations investigated are of the same origin in all samples investigated.

While our experiments constitute, to the best of our knowledge, the first ps time-resolved mIR measurements in 2D perovskites, a variety of time-resolved measurements on BAPI as well as on other, in some aspects similar, systems have been reported. In many cases, the vis-TA signal has been attributed to excitonic effects. In particular, multiexponential fits have been interpreted assuming different exciton recombination channels.[20,21] While vis-TA is sensible for all charge carriers, TRPL investigates only the excitonic charge carriers. Similarly, multiexponential fits with different recombination times for free and trapped processes have been proposed.[19,50] For both methods, additional bimolecular processes due to EEA have been reported at higher excitation densities.[22,51,52]

Recently, a series of publications casted some doubt on the assumption that the charge carriers in popular 2D perovskites are of a predominantly excitonic nature. In a study of the exciton spin dynamics of 2D $CsPbBr_3$ nanoplates, Tao et al. found a very weak exciton–exciton interaction and an increasing exciton spin lifetime with higher temperature.[26] They interpret their findings as effects of a polaronic screening of excitonic charge carriers, yielding exciton polarons having a considerably decreased binding energy compared to the excitonic state. Similarly, Mondal et al. showed in a combination of TRPL and vis-TA experiments that higher temperatures favor the formation of larger-size, geminate pairs with smaller binding energy in 2D systems.[53] They argue that the loosely bound species can act as a reservoir for exciton formation and subsequent recombination. The argument that exciton polarons play a significant role in the photophysics of 2D perovskites has also been stressed by Srimath Kandada and Silva.[54]

In a recent article, Simbula et al. investigated a wide range of perovskites by analyzing their vis-TA and TRPL signal in a tandem spectroscopy setup.[23] They found that in all systems investigated, including some 2D perovskites such as $(BA)_2PbI_4$, excitons form the minority charge carrier with dark, nonluminescent species being the majority charge carriers. They interpreted their findings as polarons occurring in the form of a polaron plasma, which is in a dynamic equilibrium with bound excitons. Using a rate model, they argue that the majority photoexcitations, being described as polarons, replenish decayed excitons, which form the main recombination channel visible by TRPL measurements. Therefore, a bimolecular recombination behavior present in a vis-TA signal can be

https://doi.org/10.1021/acs.jpclett.1c03099
J. Phys. Chem. Lett. 2021, 12, 10450–10456

associated with the formation of excitons from dark states, which thereafter produce a characteristic excitonic emission signal. Thus, the excitonic decay is driven by the changes in the dark reservoir charge-carrier density.

While an analysis of vis-TA data together with appropriate TRPL measurements allows only indirect conclusions on the dark-state population, the mIR measurements presented in our article are particularly and directly sensitive to screened charge carriers with a reduced binding energy. We find the results of our mIR-TA measurements in combination with steady-state PL analysis in very good agreement with the recent publications implying screened species to play a very important role in the photophysics of 2D perovskites. In particular, we can associate the bimolecular recombination mechanism clearly visible in all $(BA)_2(MA)_{n-1}Pb_nI_{3n+1}$ (n = 1, 2, 3) with nongeminate exciton formation from a dark majority species with a strong electron−phonon coupling leading to a reduced binding energy. We additionally find from the steady-state PL spectra that the concluding recombination step is of excitonic nature. Using a rate model for a predominantly screened carrier population in equilibrium with excitons, we interpret our steady-state PL excitation power dependence as a direct result of this combined recombination path. We find that the change in recombining excitons $\dot{n}_x$, which is proportional to the steady-state photoluminescence signal, scales with the amount of additional photoexcitations created on the sample $\dot{n}_{sc}$, being proportional to increases in the excitation density, according to a power law with an exponent of 1.5, similar to our findings present above.

Our assignment of the mIR-TA signal to a dark, screened species is further strengthened, as there are no relevant differences in the bimolecular recombination behavior for the three active layer thicknesses n, which are associated with exciton energies above or around the probe energy, investigated. The lack of polaron-associated IRAV modes further implies that the charge carriers monitored here are not of purely polaronic nature either.

Using time-resolved mIR spectroscopy, we demonstrate that dark, screened charge-carriers with polaronic properties play an important role in the model $(BA)_2(MA)_{n-1}Pb_nI_{3n+1}$ (n = 1, 2, 3) 2D perovskites. We find that these photoexcitations recombine bimolecularly independent of layer thickness. From our steady-state PL experiments, we conclude that the dark states form bright excitons, which then recombine radiatively. Our experiments emphasize the important role of charge-carrier screening and the charge−lattice interaction in 2D perovskites, contributing to the ongoing debate regarding the nature of photoexcitations in Ruddlesden−Popper hybrid metal halide perovskites. Our results show that strategies for activating the dark-state population is key for producing bright luminescence, which will be desired for use of these materials in light-emitting and photonic applications.

■ ASSOCIATED CONTENT

Supporting Information

The Supporting Information is available free of charge at https://pubs.acs.org/doi/10.1021/acs.jpclett.1c03099.

Experimental methods and sample preparation; additional information on the calculation of the initial charge-carrier density n_0 and the relation between excitonic PL intensity and the excitation density. Analysis of ground-state infrared spectra, excited-state mIR spectra, UV−vis spectra with scattering effects, bi- and monomolecular fit for $(BA)_2(MA)_2Pb_3I_{10}$ data set (PDF)

■ AUTHOR INFORMATION

Corresponding Authors

Felix Deschler − *Walter Schottky Institut, Physik-Department, Technische Universität München, 85748 Garching, Germany;* orcid.org/0000-0002-0771-3324; Email: felix.deschler@wsi.tum.de

Hristo Iglev − *Lehrstuhl für Laser- und Röntgenphysik, Physik-Department, Technische Universität München, 85748 Garching, Germany;* orcid.org/0000-0001-9208-0068; Email: higlev@ph.tum.de

Authors

Matthias Nuber − *Lehrstuhl für Laser- und Röntgenphysik, Physik-Department, Technische Universität München, 85748 Garching, Germany;* orcid.org/0000-0002-4409-3590

Daniel Sandner − *Lehrstuhl für Laser- und Röntgenphysik, Physik-Department, Technische Universität München, 85748 Garching, Germany*

Timo Neumann − *Cavendish Laboratory, University of Cambridge, Cambridge CB30HE, U.K.; Walter Schottky Institut, Physik-Department, Technische Universität München, 85748 Garching, Germany*

Reinhard Kienberger − *Lehrstuhl für Laser- und Röntgenphysik, Physik-Department, Technische Universität München, 85748 Garching, Germany*

Complete contact information is available at: https://pubs.acs.org/10.1021/acs.jpclett.1c03099

Notes

The authors declare no competing financial interest.

■ ACKNOWLEDGMENTS

This research was supported by the Deutsche Forschungsgemeinschaft (DFG) via the Cluster of Excellence "e-conversion" EXC 2089/1-390776260. M.N. thanks the "Studienstiftung des deutschen Volkes" for a PhD scholarship. F.D. acknowledges funding from the DFG Emmy Noether Program.

■ REFERENCES

(1) Rajagopal, A.; Yao, K.; Jen, A. K.-Y. Toward Perovskite Solar Cell Commercialization: A Perspective and Research Roadmap Based on Interfacial Engineering. *Adv. Mater.* **2018**, *30*, No. 1800455.

(2) Correa-Baena, J.-P.; Saliba, M.; Buonassisi, T.; Grätzel, M.; Abate, A.; Tress, W.; Hagfeldt, A. Promises and Challenges of Perovskite Solar Cells. *Science* **2017**, *358*, 739−744.

(3) Stranks, S. D.; Hoye, R. L. Z.; Di, D.; Friend, R. H.; Deschler, F. The Physics of Light Emission in Halide Perovskite Devices. *Adv. Mater.* **2019**, *31*, No. 1803336.

(4) Cortecchia, D.; Yin, J.; Petrozza, A.; Soci, C. White Light Emission in Low-Dimensional Perovskites. *J. Mater. Chem. C* **2019**, *7*, 4956−4969.

(5) Leung, S.-F.; Ho, K.-T.; Kung, P.-K.; Hsiao, V. K. S.; Alshareef, H. N.; Wang, Z. L.; He, J.-H. A Self-Powered and Flexible Organometallic Halide Perovskite Photodetector with Very High Detectivity. *Adv. Mater.* **2018**, *30*, 1704611.

(6) Fu, Q.; Wang, X.; Liu, F.; Dong, Y.; Liu, Z.; Zheng, S.; Chaturvedi, A.; Zhou, J.; Hu, P.; Zhu, Z.; et al. Ultrathin Ruddlesden-Popper Perovskite Heterojunction for Sensitive Photodetection. *Small* **2019**, *15*, No. 1902890.

(7) Munson, K. T.; Kennehan, E. R.; Doucette, G. S.; Asbury, J. B. Dynamic Disorder Dominates Delocalization, Transport, and Recombination in Halide Perovskites. *Chem.* **2018**, *4*, 2826−2843.
(8) Zhu, H.; Miyata, K.; Fu, Y.; Wang, J.; Joshi, P. P.; Niesner, D.; Williams, K. W.; Jin, S.; Zhu, X.-Y. Screening in Crystalline Liquids Protects Energetic Carriers in Hybrid Perovskites. *Science* **2016**, *353*, 1409−1413.
(9) Tan, H.; Che, F.; Wei, M.; Zhao, Y.; Saidaminov, M. I.; Todorović, P.; Broberg, D.; Walters, G.; Tan, F.; Zhuang, T.; et al. Dipolar Cations Confer Defect Tolerance in Wide-Bandgap Metal Halide Perovskites. *Nat. Commun.* **2018**, *9*, 3100.
(10) Joshi, P. P.; Maehrlein, S. F.; Zhu, X. Dynamic Screening and Slow Cooling of Hot Carriers in Lead Halide Perovskites. *Adv. Mater.* **2019**, *31*, No. 1803054.
(11) Ghosh, D.; Welch, E.; Neukirch, A. J.; Zakhidov, A.; Tretiak, S. Polarons in Halide Perovskites: A Perspective. *J. Phys. Chem. Lett.* **2020**, *11*, 3271−3286.
(12) Zheng, F.; Wang, L. Large Polaron Formation and Its Effect on Electron Transport in Hybrid Perovskites. *Energy Environ. Sci.* **2019**, *12*, 1219−1230.
(13) Nan, G.; Beljonne, D.; Zhang, X.; Quarti, C. Organic Cations Protect Methylammonium Lead Iodide Perovskites Against Small Exciton-Polaron Formation. *J. Phys. Chem. Lett.* **2020**, *11*, 2983−2991.
(14) Dunfield, S. P.; Bliss, L.; Zhang, F.; Luther, J. M.; Zhu, K.; Hest, M. F. A. M.; Reese, M. O.; Berry, J. J. From Defects to Degradation: A Mechanistic Understanding of Degradation in Perovskite Solar Cell Devices and Modules. *Adv. Energy Mater.* **2020**, *10*, 1904054.
(15) Boyd, C. C.; Cheacharoen, R.; Leijtens, T.; McGehee, M. D. Understanding Degradation Mechanisms and Improving Stability of Perovskite Photovoltaics. *Chem. Rev.* **2019**, *119*, 3418−3451.
(16) Brennan, M. C.; Ruth, A.; Kamat, P. V.; Kuno, M. Photoinduced Anion Segregation in Mixed Halide Perovskites. *Trends in Chemistry* **2020**, *2*, 282−301.
(17) Chen, Y.; Sun, Y.; Peng, J.; Tang, J.; Zheng, K.; Liang, Z. 2D Ruddlesden-Popper Perovskites for Optoelectronics. *Adv. Mater.* **2018**, *30*, 1703487.
(18) Buizza, L. R. V.; Herz, L. M. Polarons and Charge Localization in Metal-Halide Semiconductors for Photovoltaic and Light-Emitting Devices. *Adv. Mater.* **2021**, *33*, No. 2007057.
(19) Yin, T.; Liu, B.; Yan, J.; Fang, Y.; Chen, M.; Chong, W. K.; Jiang, S.; Kuo, J.-L.; Fang, J.; Liang, P.; et al. Pressure-Engineered Structural and Optical Properties of Two-Dimensional (C4H9NH3)-2PbI4 Perovskite Exfoliated Nm-Thin Flakes. *J. Am. Chem. Soc.* **2019**, *141*, 1235−1241.
(20) Bakthavatsalam, R.; Biswas, A.; Chakali, M.; Bangal, P. R.; Kore, B. P.; Kundu, J. Temperature-Dependent Photoluminescence and Energy-Transfer Dynamics in Mn 2+ -Doped (C 4 H 9 NH 3) 2 PbBr 4 Two-Dimensional (2D) Layered Perovskite. *J. Phys. Chem. C* **2019**, *123*, 4739−4748.
(21) Wu, X.; Trinh, M. T.; Zhu, X.-Y. Excitonic Many-Body Interactions in Two-Dimensional Lead Iodide Perovskite Quantum Wells. *J. Phys. Chem. C* **2015**, *119*, 14714−14721.
(22) Deng, S.; Shi, E.; Yuan, L.; Jin, L.; Dou, L.; Huang, L. Long-Range Exciton Transport and Slow Annihilation in Two-Dimensional Hybrid Perovskites. *Nat. Commun.* **2020**, *11*, 664.
(23) Simbula, A.; Pau, R.; Wang, Q.; Liu, F.; Sarritzu, V.; Lai, S.; Lodde, M.; Mattana, F.; Mula, G.; Geddo Lehmann, A.; et al. Polaron Plasma in Equilibrium with Bright Excitons in 2D and 3D Hybrid Perovskites. *Adv. Opt. Mater.* **2021**, *9*, 2100295.
(24) Ivanovska, T.; Dionigi, C.; Mosconi, E.; De Angelis, F.; Liscio, F.; Morandi, V.; Ruani, G. Long-Lived Photoinduced Polarons in Organohalide Perovskites. *J. Phys. Chem. Lett.* **2017**, *8*, 3081−3086.
(25) Mahata, A.; Meggiolaro, D.; De Angelis, F. From Large to Small Polarons in Lead, Tin, and Mixed Lead-Tin Halide Perovskites. *J. Phys. Chem. Lett.* **2019**, *10*, 1790−1798.
(26) Tao, W.; Zhou, Q.; Zhu, H. Dynamic Polaronic Screening for Anomalous Exciton Spin Relaxation in Two-Dimensional Lead Halide Perovskites. *Science advances* **2020**, *6*, eabb7132.
(27) Munson, K. T.; Kennehan, E. R.; Asbury, J. B. Structural Origins of the Electronic Properties of Materials via Time-Resolved Infrared Spectroscopy. *J. Mater. Chem. C* **2019**, *7*, 5889.
(28) Stallhofer, K.; Nuber, M.; Cortecchia, D.; Bruno, A.; Kienberger, R.; Deschler, F.; Soci, C.; Iglev, H. Picosecond Charge Localization Dynamics in CH3NH3PbI3 Perovskite Probed by Infrared-Activated Vibrations. *J. Phys. Chem. Lett.* **2021**, *12*, 4428−4433.
(29) Blancon, J.-C.; Tsai, H.; Nie, W.; Stoumpos, C. C.; Pedesseau, L.; Katan, C.; Kepenekian, M.; Soe, C. M. M.; Appavoo, K.; Sfeir, M. Y.; et al. Extremely Efficient Internal Exciton Dissociation Through Edge States in Layered 2D Perovskites. *Science* **2017**, *355*, 1288−1292.
(30) Cao, D. H.; Stoumpos, C. C.; Farha, O. K.; Hupp, J. T.; Kanatzidis, M. G. 2D Homologous Perovskites as Light-Absorbing Materials for Solar Cell Applications. *J. Am. Chem. Soc.* **2015**, *137*, 7843−7850.
(31) Thouin, F.; Neutzner, S.; Cortecchia, D.; Dragomir, V. A.; Soci, C.; Salim, T.; Lam, Y. M.; Leonelli, R.; Petrozza, A.; Kandada, A. R. S. Stable Biexcitons in Two-Dimensional Metal-Halide Perovskites with Strong Dynamic Lattice Disorder. *Phys. Rev. Materials* **2018**, *2*, 034001.
(32) Li, W.; Ma, J.; Wang, H.; Fang, C.; Luo, H.; Li, D. Biexcitons in 2D (Iso-BA)2PbI4 Perovskite Crystals. *Nanophotonics* **2020**, *9*, 2001−2006.
(33) Shang, Q.; Wang, Y.; Zhong, Y.; Mi, Y.; Qin, L.; Zhao, Y.; Qiu, X.; Liu, X.; Zhang, Q. Unveiling Structurally Engineered Carrier Dynamics in Hybrid Quasi-Two-Dimensional Perovskite Thin Films Toward Controllable Emission. *J. Phys. Chem. Lett.* **2017**, *8*, 4431−4438.
(34) Zheng, K.; Chen, Y.; Sun, Y.; Chen, J.; Chábera, P.; Schaller, R.; Al-Marri, M. J.; Canton, S. E.; Liang, Z.; Pullerits, T. Inter-Phase Charge and Energy Transfer in Ruddlesden−Popper 2D Perovskites: Critical Role of the Spacing Cations. *J. Mater. Chem. A* **2018**, *6*, 6244−6250.
(35) Schmidt, T.; Lischka, K.; Zulehner, W. Excitation-Power Dependence of the Near-Band-Edge Photoluminescence of Semiconductors. *Phys. Rev. B: Condens. Matter Mater. Phys.* **1992**, *45*, 8989−8994.
(36) Yi, H. T.; Irkhin, P.; Joshi, P. P.; Gartstein, Y. N.; Zhu, X.; Podzorov, V. Experimental Demonstration of Correlated Flux Scaling in Photoconductivity and Photoluminescence of Lead-Halide Perovskites. *Phys. Rev. Appl.* **2018**, *10*, 054016.
(37) Gan, L.; Li, J.; Fang, Z.; He, H.; Ye, Z. Effects of Organic Cation Length on Exciton Recombination in Two-Dimensional Layered Lead Iodide Hybrid Perovskite Crystals. *J. Phys. Chem. Lett.* **2017**, *8*, 5177−5183.
(38) Zhang, Y.; Wang, R.; Li, Y.; Wang, Z.; Hu, S.; Yan, X.; Zhai, Y.; Zhang, C.; Sheng, C. Optical Properties of Two-Dimensional Perovskite Films of (C6H5C2H4NH3)2PbI4 and (C6H5C2H4NH3)2 (CH3NH3)2Pb3I10. *J. Phys. Chem. Lett.* **2019**, *10*, 13−19.
(39) Linnenbank, H.; Saliba, M.; Gui, L.; Metzger, B.; Tikhodeev, S. G.; Kadro, J.; Nasti, G.; Abate, A.; Hagfeldt, A.; Graetzel, M.; et al. Temperature Dependent Two-Photon Photoluminescence of CH 3 NH 3 PbBr 3 Structural Phase and Exciton to Free Carrier Transition. *Opt. Mater. Express* **2018**, *8*, 511.
(40) Gautam, S. K.; Kim, M.; Miquita, D. R.; Bourée, J.-E.; Geffroy, B.; Plantevin, O. Reversible Photoinduced Phase Segregation and Origin of Long Carrier Lifetime in Mixed-Halide Perovskite Films. *Adv. Funct. Mater.* **2020**, *30*, 2002622.
(41) Saba, M.; Cadelano, M.; Marongiu, D.; Chen, F.; Sarritzu, V.; Sestu, N.; Figus, C.; Aresti, M.; Piras, R.; Lehmann, A. G.; et al. Correlated Electron-Hole Plasma in Organometal Perovskites. *Nat. Commun.* **2014**, *5*, 5049.
(42) Draguta, S.; Thakur, S.; Morozov, Y. V.; Wang, Y.; Manser, J. S.; Kamat, P. V.; Kuno, M. Spatially Non-Uniform Trap State Densities in Solution-Processed Hybrid Perovskite Thin Films. *J. Phys. Chem. Lett.* **2016**, *7*, 715−721.

https://doi.org/10.1021/acs.jpclett.1c03099
J. Phys. Chem. Lett. 2021, 12, 10450−10456

(43) Liu, Q.; Chen, H.; Wang, Z.; Weng, Y. Observation of the Polaron Excited State in a Single-Crystal ZnO. *J. Phys. Chem. C* **2021**, *125*, 10274−10283.
(44) Munson, K. T.; Doucette, G. S.; Kennehan, E. R.; Swartzfager, J. R.; Asbury, J. B. Vibrational Probe of the Structural Origins of Slow Recombination in Halide Perovskites. *J. Phys. Chem. C* **2019**, *123*, 7061−7073.
(45) Blancon, J.-C.; Stier, A. V.; Tsai, H.; Nie, W.; Stoumpos, C. C.; Traoré, B.; Pedesseau, L.; Kepenekian, M.; Katsutani, F.; Noe, G. T.; et al. Scaling Law for Excitons in 2D Perovskite Quantum Wells. *Nat. Commun.* **2018**, *9*, 2254.
(46) Herz, L. M. How Lattice Dynamics Moderate the Electronic Properties of Metal-Halide Perovskites. *J. Phys. Chem. Lett.* **2018**, *9*, 6853−6863.
(47) Herz, L. M. Charge-Carrier Dynamics in Organic-Inorganic Metal Halide Perovskites. *Annu. Rev. Phys. Chem.* **2016**, *67*, 65−89.
(48) deQuilettes, D. W.; Frohna, K.; Emin, D.; Kirchartz, T.; Bulovic, V.; Ginger, D. S.; Stranks, S. D. Charge-Carrier Recombination in Halide Perovskites. *Chem. Rev.* **2019**, *119*, 11007−11019.
(49) Chen, X.; Lu, H.; Li, Z.; Zhai, Y.; Ndione, P. F.; Berry, J. J.; Zhu, K.; Yang, Y.; Beard, M. C. Impact of Layer Thickness on the Charge Carrier and Spin Coherence Lifetime in Two-Dimensional Layered Perovskite Single Crystals. *ACS Energy Lett.* **2018**, *3*, 2273−2279.
(50) Zhou, C.; Chen, W.; Yang, S.; Ou, Q.; Gan, Z.; Bao, Q.; Jia, B.; Wen, X. Determining in-Plane Carrier Diffusion in Two-Dimensional Perovskite Using Local Time-Resolved Photoluminescence. *ACS Appl. Mater. Interfaces* **2020**, *12*, 26384−26390.
(51) Delport, G.; Chehade, G.; Lédée, F.; Diab, H.; Milesi-Brault, C.; Trippé-Allard, G.; Even, J.; Lauret, J.-S.; Deleporte, E.; Garrot, D. Exciton-Exciton Annihilation in Two-Dimensional Halide Perovskites at Room Temperature. *J. Phys. Chem. Lett.* **2019**, *10*, 5153−5159.
(52) Burgos-Caminal, A.; Socie, E.; Bouduban, M. E. F.; Moser, J.-E. Exciton and Carrier Dynamics in Two-Dimensional Perovskites. *J. Phys. Chem. Lett.* **2020**, *11*, 7692−7701.
(53) Mondal, N.; Naphade, R.; Zhou, X.; Zheng, Y.; Lee, K.; Gereige, I.; Al-Saggaf, A.; Bakr, O. M.; Mohammed, O. F.; Gartstein, Y. N.; et al. Dynamical Interconversion Between Excitons and Geminate Charge Pairs in Two-Dimensional Perovskite Layers Described by the Onsager-Braun Model. *J. Phys. Chem. Lett.* **2020**, *11*, 1112−1119.
(54) Srimath Kandada, A. R.; Silva, C. Exciton Polarons in Two-Dimensional Hybrid Metal-Halide Perovskites. *J. Phys. Chem. Lett.* **2020**, *11*, 3173−3184.

https://doi.org/10.1021/acs.jpclett.1c03099
J. Phys. Chem. Lett. 2021, 12, 10450−10456